Measurement of incoming radiation below forest canopies: A comparison of different radiometer configurations

Clare Webster[1,2*], Nick Rutter[1], Franziska Zahner[2,3], Tobias Jonas[2]

[1] Department of Geography, Faculty of Engineering and Environment, Northumbria University, Newcastle upon Tyne, NE1 8ST UK

[2] WSL Institute for Snow and Avalanche Research SLF, CH-7260 Davos Dorf, Switzerland

[3] Institute of Environmental Engineering, ETH Zurich, Switzerland

Correspondence to: C. Webster, clare.webster@northumbria.ac.uk, Tel: +44 191 227 4294

ABSTRACT

Ground-based, sub-canopy measurements of incoming shortwave and longwave radiation are frequently used to drive and validate energy balance and snowmelt models. These sub-canopy measurements are frequently obtained using different configurations (linear or distributed; stationary or moving) of radiometer arrays that are installed to capture the spatial and temporal variability of longwave and shortwave radiation. Three different radiometer configurations (stationary distributed, stationary linear and moving linear) were deployed in a spruce forest in the eastern Swiss Alps across a 9 month period, capturing the annual range of sun angles and sky conditions. Results showed a strong seasonal variation in differences between measurements of shortwave transmissivity between the three configurations whereas differences in longwave enhancement appeared to be seasonally independent. Shortwave transmissivity showed a larger spatial variation in the sub-canopy than longwave enhancement at this field site. The two linear configurations showed the greatest similarity in shortwave transmissivity measurements and the measurements of longwave enhancement were

largely similar between all three configurations. A reduction in the number of radiometers in each array reduced the similarities between each stationary configuration. The differences presented here are taken to reflect the natural threshold of spatial noise in sub-canopy measurements that can be expected between the three configurations.

Keywords: Canopy radiative transfer; radiometer configuration; shortwave transmissivity; longwave enhancement; coniferous forest; hemispherical photography

INTRODUCTION

Total incoming radiation is the dominant component in the sub-canopy energy balance. Incoming sub-canopy radiation is comprised of shortwave and longwave radiation, both of which are modified by the overlying canopy structure, creating strong spatial and temporal variations different to those seen above the canopy or in adjacent open areas (Baldocchi et al. 2000; Harding and Pomeroy 1996; Lundquist et al. 2013). Understanding how the canopy structure controls the transmissivity of shortwave radiation and the enhancement of longwave radiation is therefore important for driving sub-canopy net radiation energy balance and snowmelt models (Hardy et al. 2004).

The strong spatial and temporal variability of sub-canopy shortwave and longwave radiation means that a single fixed radiometer is not sufficient to adequately capture the sub-canopy radiative regime (Essery et al. 2008b; Link et al. 2004). Previous studies have therefore deployed arrays of 10 or more radiometers in one of three radiometer configurations (stationary distributed, stationary linear and moving linear). For example, Essery et al. (2008a) and Reid et al. (2014) used data collected from stationary linear and distributed radiometer configurations, respectively, to drive and validate longwave and shortwave radiation models, respectively. Distributed arrays are usually located either

randomly (e.g. Essery et al. 2008a; Hardy et al. 1998), by selection of random grid or azimuth (e.g. Link et al. 2004; Pomeroy et al. 2009) or by a pre-determined pattern independent of human-induced bias (e.g. Reid et al. 2014). Linear arrays have been used previously to assess or characterize variation across a canopy discontinuity. Stationary (e.g. Ellis et al. 2013; Essery et al. 2008a; Lawler and Link 2011) and moving (e.g. Stähli et al. 2009) linear arrays have been installed to measure incoming shortwave and longwave radiation with the aim of improving understanding of influences of forest structure on sub-canopy radiation dynamics across different sized gaps in the canopy. In addition to the study by Stähli et al. (2009), moving linear configurations have also been adopted by Black et al. (1991), Chen et al. (1997), Law et al. (2001), Blanken et al. (2001) and Vrugt et al. (2002), however this method was only employed in warmer months when the rail and radiometer was not affected by icing and snowfall (Link et al. 2004).

Whilst many different radiometer configurations are possible, radiation measurements from these three different configurations (stationary distributed, stationary linear and moving linear) have been widely used to characterize sub-canopy radiation and develop snowmelt and energy transfer models (e.g. Essery et al. 2008a; Essery et al. 2009; Lawler and Link 2011; Link et al. 2004; Pomeroy et al. 2009; Reid et al. 2014; Sicart et al. 2004; Stähli et al. 2009). There is difficulty, however, in comparing radiation measurements and modeling results from different sites, locations and radiometer configurations due to strong spatial variation in sub-canopy incoming shortwave and longwave radiation (Essery et al. 2008b). In particular, how these three selected configurations perform relative to each other in how they capture the sub-canopy radiation variability has not yet been assessed.

This paper compares sub-canopy incoming longwave and shortwave radiation measurements from three different radiometer configurations (stationary distributed, stationary linear and moving linear)

across four different periods of an annual cycle in the same sub-canopy environment. The aim of this investigation is to evaluate the spatial and temporal variability in differences between the measured sub-canopy longwave and shortwave radiation by each configuration. In addition, further analysis subsets the number of radiometers in each configuration to assess the performance of smaller arrays compared to the larger arrays in representing the sub-canopy radiative regime. Results from this analysis will demonstrate the capabilities of each configuration to capture the spatial and temporal variability in incoming sub-canopy shortwave and longwave radiation.

STUDY SITE

The Seehornwald measurement site (46°48'55" N, 9°51'21" E) is located at 1640 m a.s.l., near Davos, Switzerland, in the central European Alps and is an established field site of the Swiss Federal Institute for Forest, Snow and Landscape Research, WSL. The coniferous forest is dominated by Norwegian Spruce trees, which reach a maximum stand height of 27 m, and have an average leaf area index of 3.9 m^2 m^{-2}.

METHODS

Longwave and shortwave radiation

This study compared measurements from three different radiometer configurations: a moving rail, a stationary linear configuration parallel to the rail and a distributed configuration on the forest floor. Simultaneous above-canopy measurements were obtained on top of a 35 m high tower approximately 8 m above the forest canopy.

87 Non-ventilated Kipp and Zonen CNR1 net radiometer sensors were mounted on both the moving rail
88 (sub-canopy) and at a fixed position on the tower (above canopy), which measured incoming and
89 outgoing longwave and shortwave radiation at a 15 second resolution. Details of the rail mounted
90 radiometers and setup were the same as that described in Stähli et al. (2009), which was moved from
91 the Alptal site to the current Seehornwald site in 2007. The sub-canopy CNR1 moved along a 10m
92 heated rail at 10-minute intervals at a constant rate, at a height of approximately 2 m above the forest
93 floor. The rail moves from a relatively closed canopy (sky view factor (SVF) = 0.02) next to a tree
94 trunk into an area below a small gap in the forest canopy (SVF = 0.05). In addition to measurements
95 of radiation, sensor position along the rail was recorded every 15 seconds, resulting in 40 different
96 radiation measurements at approximately 25 cm intervals along the rail for each 10 minute period.

97 The linear and distributed stationary configurations consisted of different instruments than the
98 moving linear configuration: ten Kipp and Zonen CMP3 shortwave radiation pyranometers and four
99 Kipp and Zonen CGR3 longwave radiation pyrgeometers. In the linear configuration, pyranometers
100 were installed at 1 m intervals and pyrgeometers at 2 m intervals along a wooden plank parallel to the
101 rail and at the same height above the ground (Figure 1). Radiometers in the distributed configuration
102 were leveled on small wooden platforms on the forest floor at positions that covered a range of SVFs.
103 These locations were subjectively selected visually with the aim of positioning them within the same
104 range of SVFs represented by the linear configuration and moving rail (range of SVF from 0.02 to
105 0.05). Ranges in SVF for the distributed configuration were 0.02 to 0.05 (with one value of 0.09).
106 The two stationary arrays were each connected to Campbell Scientific CR1000 data loggers that
107 recorded measurements at 15-second intervals.

108 The linear and distributed configurations were installed between October – December 2013 and May
109 – June 2014. Where overlapping data allowed, four different analysis periods were selected in order

to capture the annual range of sun angles, above canopy meteorological conditions and snowpack states (accumulation and melt). Analysis periods were October 2013 (autumn), December 2013 (winter), May 2014 (spring) and June 2014 (summer) (see Table 1 for further details). Due to instrument failure, incoming longwave radiation data from the rail were not available for the autumn analysis period, and the distributed configuration in the spring and summer analysis periods consisted of nine rather than ten shortwave sensors.

Throughout the measurement periods, sensors were checked, cleaned and leveled immediately following precipitation events, and every second day during dry periods. The rail had a brush installed at one end that cleared precipitation and debris from the top of the CNR1 sensors as they passed underneath every 10 minutes. The rail was also heated to prevent freezing during colder periods.

Forest canopy structure

Sky-view factor above each sensor was determined using hemispherical photographs taken at the exact locations of the 14 sensors in the stationary linear and distributed configurations, 15 cm above the sensor heights, using a Canon 600D digital camera with a Sigma 4.5 mm fish-eye lens. The camera was attached to a specifically designed steel plate fitted with spirit level and compass to enable accurate leveling and post-processing corrections from magnetic north to true north (eliminating the influence of the metal rail on the compass accuracy). All photos were taken during February 2014 on suitably overcast days. Differences in horizontal position of the stationary linear configuration sensors relative to the CNR1 sensor on the rail were no more than 20 cm and therefore it was assumed that the distribution of sky-view factors along the two linear configurations did not significantly deviate from each other.

Data quality control, post-processing and analytical methods

A CNR1 consists of two CM3 pyranometers and two CG3 pyrgeometers, which are the predecessors of the CGR3 and CMP3 radiometers used in the two stationary configurations. Individual pyranometers and pyrgeometers on the two CNR1 net radiometers on the sub-canopy rail and the tower were calibrated outdoors by the World Radiation Centre in Davos, Switzerland, to World Radiation Centre standards (Fröhlich 1977) during August 2013. The pyranometers and pyrgeometers in the two stationary configurations were factory calibrated in November 2010 to ISO 9060 calibration standard. Additional open-site comparison of the sensors in the two stationary configurations was carried out in January 2014 and all were found to measure within 7 Wm^{-2} for the pyrgeometers and 1 Wm^{-2} for the pyranometers. Further data quality control procedures included manually removing all data that was affected by either human interference, precipitation on the surface or tilting of the sensors. Night-time measurements of incoming shortwave radiation were also excluded from the statistical analysis as they would unfairly reduce daytime biases.

To make results transferable to different altitudes and latitudes, above canopy data from the tower were used to calculate shortwave transmissivity and longwave enhancement below the canopy. These dimensionless values describe the proportion of incoming radiation that reaches the forest floor compared to that measured above the canopy, represented as a ratio between above and below canopy measured radiation.

Three different comparisons were conducted between individual configurations using data averaged to 10-minute resolution, as this is the period of time it took for the CNR1 to travel one full length of the rail. For the two stationary configurations, 10-minute averages were calculated for each sensor and one average value was then calculated for each sensor type. This resulted in one incoming

154 longwave and shortwave radiation value for each configuration. Data from the moving linear
155 configuration were averaged over the 10-minute period taken to cover the length of the rail.

156 Often the installation of 14 sensors under a forest canopy is not possible due to reasons such as
157 accessibility or equipment availability. In response to this common problem, three pyranometers and
158 one pyrgeometer from each of the stationary configurations were selected and averaged. Sensors in
159 this smaller subset were selected subjectively in order to maintain the full range of SVFs that are
160 represented by the larger configurations. Pyranometers with the largest, median and lowest SVFs
161 were selected for further analysis. In the linear configuration, these were SW10, SW1 and SW8; in
162 the distributed configuration these were SW5, SW7 and SW10 (Figure 1). The LW3 sensor was
163 selected in both configurations as these were visually determined to be located in positions very close
164 to the median SVF for each configuration.

165 SVFs were derived from hemi-photos following Schleppi et al. (2007) using *Hemisfer,* version 1.5.3.
166 Binary classification of pixels in hemi-photos are divided into concentric rings based on elevation
167 angle (θ) and images were classified as either white (sky) or black (canopy) by applying a brightness
168 threshold using the algorithm of Nobis and Hunziker (2005). Sky-view factor was calculated by the
169 ratio between numbers of sky and canopy pixels in each concentric ring, weighted by elevation angle
170 (Essery et al. 2008a).

171 The impact of radiometer configurations on measurements of sub-canopy shortwave transmissivity
172 and longwave enhancement was quantified using three different statistical indicators. The degree of
173 difference between the configurations in each comparison was determined by calculating the mean of
174 the differences between measurements and the coefficient of variation of these differences was
175 calculated to indicate the variability in the distribution. The linear correlation between configurations
176 was characterized using the Pearson's correlation coefficient (R).

177 **RESULTS**

178 Sky-view factors in all three configurations ranged from 0.02 to 0.05, with one outlying value of 0.09
179 in the distributed configuration. A Wilcoxon rank sum test identified no statistical difference between
180 the two configurations (p-values of 0.21 and 0.49 for the pyranometers and pyrgeometers,
181 respectively). Differences between these SVFs of the configurations show that due to high spatial
182 variability of the canopy, it is not possible to gain identical values between configurations. However,
183 SVFs do not differ greatly, and thus a natural variability in SVF was obtained that is representative of
184 different sub-canopy sensor configurations in uniformly dense environments.

185 Differences in measurements of shortwave transmissivity and longwave enhancement by the three
186 configurations are shown in Figure 2. Incoming sub-canopy shortwave radiation in the Seehornwald
187 forest was reduced by over 60% beneath the forest canopy, with the shortwave transmissivities
188 ranging from 0 to 38%. Transmissivities were highest in summer, when peak daytime values were
189 between 12 and 38% compared to those measured in winter where the maximum measured daily
190 transmissivity was 0.11. The opposite pattern was seen in the measurements of longwave
191 enhancement, which were highest in autumn and winter (maximum of 158 and 146%, respectively)
192 compared to spring and summer (maximum of 140 and 138%, respectively).

193 Statistical analyses of the three comparisons also showed seasonal variation, particularly in
194 shortwave transmissivity measurements (Figure 3). Both the mean and the coefficient of variation
195 (CV) of the differences between transmissivity measurements were lowest in the autumn and winter
196 (mean differences ranged between 0.8 and 1.6 % measured transmissivity) and linear correlations
197 were stronger between the configurations in these seasons (*R*-values*:* 0.891 to 0.953). All *R*-values
198 were statistically significant at 99% confidence. Greater variability of shortwave transmissivity from
199 winter to summer is shown by CVs of the differences (Figure 3), which were lowest in winter

200 (between 78 and 88%) compared to summer when CVs were almost double (between 115 and
201 167%). These values indicate differences between the configurations can vary by up to 167% during
202 summer and 88% in winter. Mean differences in shortwave transmissivity between configurations
203 were all below 3% showing that, on average, all configurations were measuring shortwave
204 transmissivity within this range.

205 Unlike the comparisons of shortwave transmissivity measurements, statistical results of the longwave
206 enhancement comparisons showed less seasonal variation in all three comparisons (Figure 3). For
207 each comparison, mean differences were below 0.5% (distributed vs. stationary linear) and 1.8%
208 (stationary linear and stationary distributed vs. rail) of measured longwave enhancement in all four
209 seasons and *R*-values were all above 0.99 and statistically significant at 99% confidence. Lower
210 coefficients of variation in all four seasons and in all three comparisons of longwave enhancement
211 than those in the shortwave transmissivity comparisons (Figure 3) indicate a smaller spread in the
212 distribution of differences between measurements of enhancement compared to those of
213 transmissivity.

214 Out of the three comparisons of radiometer configurations, shortwave transmissivity measurements
215 showed greatest agreement between the two linear configurations in all four seasons, shown by mean
216 differences between 0.8 and 1.8% of measured shortwave transmissivity. In contrast, mean
217 differences for the comparison between the rail and distributed configurations were between 0.9 and
218 2.7%. Measurements between the two comparisons with the stationary linear configuration correlated
219 well, with statistically significant *R*-values above 0.8, excluding the comparison between the two
220 stationary configurations in summer ($R = 0.64$). High *R*-values and low mean differences show that
221 while not picking up identical spatial patterns, temporal patterns were well represented between the
222 two configurations.

223 Statistical results from the three comparisons show that the stationary and moving linear
224 configurations had the greatest similarities in measurements of shortwave transmissivity whereas the
225 two stationary configurations showed the greatest similarities in measurements of longwave
226 enhancement (Figure 3). All three comparisons of longwave enhancement had *R*-values within 1% of
227 a perfect correlation, but mean differences were higher in the two comparisons involving the moving
228 rail (Figure 3), which used the CNR1 instead of the CGR3 pyrgeometers. Mean differences for the
229 comparison between the two stationary configurations were below 3.3% in all seasons. Comparisons
230 involving the moving rail show an offset in measurements, with the rail measuring lower
231 enhancements than the two stationary configurations in all seasons (Figure 2), a difference which
232 corresponds to a maximum of approximately 6 Wm^{-2}. Both comparisons with the moving rail had
233 mean differences between 2.8 and 3.1% of enhancement and CVs between 14 and 22% (Figure 3).

234 Increasing the averaging time from 10 minutes to one hour reduced the mean difference and
235 coefficients of variation in the shortwave transmissivity comparisons. All three comparisons showed
236 similar decreases, which were largest in summer and smallest in winter. Overall mean differences
237 decreased by a maximum of 0.5% transmissivity. Averaging over a one hour period showed no
238 reduction in mean difference or variation in the measurements of longwave enhancement between the
239 three configurations.

240 Reduction in the number of pyranometers in each stationary configuration from ten to three increased
241 the mean differences in all three comparisons of shortwave transmissivity in all four seasons,
242 particularly in spring and summer, and CVs increased between 6 and 27% (Figures 4 and 5). Smaller
243 increases in mean differences occurred in the comparison between the moving linear and distributed
244 configurations compared to the other two comparisons, but changes in mean differences were no
245 higher than 1.5% of measured transmissivity in all comparisons. *R*-values between transmissivity

measurements decreased, which is shown in the larger differences between measurements seen in Figure 4a, c and e, in particular all three comparisons show a pattern where one configuration measured lower transmissivity compared to the other configuration.

The changes in mean differences and CVs of longwave enhancement when configurations were reduced from four pyrgeometers to one increased in the two comparisons involving the stationary linear configuration (mean differences increased between 0.2 and 0.8%), but decreased slightly in the comparison between the distributed configuration and the moving rail. Mean differences were still highest in the two comparisons involving the moving rail (Figure 5). Overall, mean differences did not change by more than 1% enhancement (Figure 5) and linear correlations remained high (Figure 4).

DISCUSSION

The statistical results summarized in Figure 4 showed a much smaller difference in measurements of longwave enhancement between the three configurations compared to those for shortwave transmissivity in all four seasons. All comparisons of longwave enhancement had strong linear correlations (all values were over 0.998), however the longwave enhancement measured by the rail was consistently lower than that measured by the two stationary configurations (mean differences between 2.8 and 3.1% of enhancement in all seasons). This offset was no greater than 6 Wm^{-2}. The difference can be attributed to the accuracy of the CNR1 (outdoor calibrated by the World Radiation Centre in Davos, located 1km from the field site), compared to the radiometers in the stationary array that are corrected using factory calibrated sensitivity values. Additionally, comparison of all pyrgeometers in the stationary arrays was carried out in January and May 2014 and showed all sensors measure within 7 Wm^{-2}. Despite the offset, the differences are still within the error margin of the sensors in all configurations (±10%). Strong *R*-values and mean differences were all within the

269 margin of error of the instruments in all comparisons, demonstrating that all three configurations
270 captured the same spatial and temporal variability in incoming sub-canopy longwave radiation.

271 Mean differences of longwave enhancement between the three different configurations also showed a
272 much smaller degree of spatial variability compared to that seen in transmissivity. Longwave
273 enhancement has been found to exhibit strong sub-canopy spatial variability as a result of canopy
274 heating by direct insolation, which is largely restricted to times of the day when solar insolation is at
275 its highest (Essery et al. 2008a; Pomeroy et al. 2009), although variation in longwave radiation
276 measurements vary by less than 100 Wm^{-2} compared to variations of shortwave radiation in excess of
277 500 Wm^{-2}. In spite of this, however, a strong spatial variation between pyrgeometers is not seen in
278 the results from this comparison where SVFs did not greatly differ between configurations. In
279 particular, the reduction in insolation due to the low SVFs meant there was limited direct canopy
280 heating, particularly in the lower sub-canopy. Canopy emissivities also remain fixed at the stand
281 scale investigated in this study and changes in canopy and air temperatures have much smaller spatial
282 variation than solar radiation. Spatial variation in longwave enhancement was therefore smaller than
283 that of shortwave transmissivity. It is likely, however, that differences in longwave enhancement will
284 show stronger spatial variability at smaller scales, for example within one or two meters of tree
285 trunks (Woo and Giesbrecht 2000) or across canopy discontinuities (Lawler and Link 2011;
286 Rowlands et al. 2002).

287 Greater variation between measurements of shortwave transmissivity compared to those of longwave
288 enhancement were due to the spatial and temporal variation of sub-canopy sun-flecks, which have a
289 stronger influence on shortwave radiation compared to longwave. Temporal variation in incoming
290 sub-canopy shortwave radiation (from 0 Wm^{-2} at night to a peak of 900 Wm^{-2} during daytime in the
291 summer) and spatial variation in location of the sensors below the canopy lead to different intensities

292 and timing of direct insolation on the different sensors configurations. This caused increased mean
293 differences, coefficients of variation and lower *R*-values in comparisons of transmissivity between
294 sensor configurations. These larger differences and variations are more likely during clear sky
295 conditions when above canopy radiation is highest, as was shown by Rowlands et al. (2002). The
296 mean differences between configurations were no greater than 3% transmissivity, which is close to
297 the variation in measured and modeled values presented by Hardy et al. (2004). Using a mean
298 measured transmissivity and a mean modeled transmissivity that differed by 2.5%, their study
299 showed that throughout the snow season, differences in modeled snow depth diverged by less than 5
300 cm.

301 Higher midday solar angles during the spring and summer measurement periods caused higher
302 intensity of direct insolation penetrating the canopy to the forest floor, which resulted in the higher
303 spatial variation in measured shortwave transmissivity between the different sensor configurations in
304 the spring and summer seasons. The annual variation in solar angles causes further variation in
305 shortwave transmissivity values, creating differences in daily sub-canopy energy between
306 configurations which were higher in summer and spring (higher solar angles) compared to autumn
307 and winter (lower solar angles). Dependence of sub-canopy incoming shortwave radiation on solar
308 angle shows more seasonal variation than incoming longwave radiation, which is predominantly
309 controlled by forest and air temperatures that show a relatively smaller variation in energy compared
310 to solar radiation. Furthermore, when solar angles are low, canopies attenuate more solar energy, and
311 there are less direct sun-flecks reaching the forest floor than during months with higher solar angles.

312 The parallel stationary and moving linear configurations showed the greatest similarities in
313 measurements of shortwave transmissivity. Even though the SVFs of each linear configuration were
314 assumed to be identical, small-scale temporal and spatial variability of direct insolation were still

315 apparent between the configurations, particularly during periods of higher solar angles. Changes in
316 the location of the sun-flecks over the course of the day, and short-term changes due to canopy
317 movement, for example during windy periods, cause these variations in insolation at shorter time
318 scales (Reifsnyder et al. 1972). Estimates of solar transmission are therefore likely to differ greatly
319 between radiometer locations in close proximity during these periods (Brown 1973; Chazdon et al.
320 1988). However, measurements of shortwave transmissivity between the two linear configurations in
321 this study showed good agreement compared to the two comparisons involving the distributed
322 configuration.

323 Larger mean differences and smaller *R*-values in the two comparisons with the distributed
324 configuration show that increased distances between sensors result in even bigger differences in
325 measured shortwave radiation transmission, even though the distribution in SVFs were not
326 statistically significantly different. It is likely that weighting individual measurements by sky-view
327 factor at each pyranometer could further reduce these differences. Furthermore, patterns of direct
328 insolation and shade at the forest floor change throughout the daily cycle, and larger distances
329 between sensor locations results in the timing of these sun-flecks to be different for each
330 pyranometer. At larger distances between sensors, the difference between the incidences of these sun-
331 flecks on the sensors is greater, resulting in the patterns seen in Figure 2a and c where there is larger
332 variation in the two comparisons involving the distributed configuration than in the comparison
333 between the two linear configurations (Figure 2e).

334 The reduction from four to one in the number of pyrgeometers in the two stationary configurations
335 did not notably increase the differences in measurements of longwave enhancement between the
336 three configurations (Figure 2 compared to Figure 5). In particular linear correlations between the
337 two sensors with median SVFs from each stationary configuration remained strong, and mean

differences remained lower than those seen in the shortwave comparisons. These results show that in the relatively uniform canopy with low SVFs in this study, one pyrgeometer, placed in a position representative of close to average SVF, will give approximately the same information regarding temporal variability in longwave radiation that four pyrgeometers can achieve.

When the numbers of pyranometers in the stationary configurations are reduced from ten to three, mean differences in measurements of shortwave transmissivity between the three configurations increased. These larger variations were, again, more apparent in the two comparisons involving the distributed configuration. Even though the SVFs at this study plot indicate a reasonably closed canopy (SVFs varied between 0.02 and 0.05), averaging transmissivity over three sensors compared to ten increases the mean differences between configurations. This can be explained by the spatial variation caused by the distribution of sun-flecks (controlled by the spatial heterogeneity of the canopy), which is reduced by averaging over ten sensors compared to three. An increase in averaging period from 10mins to one hour in this study showed that mean differences and CVs in shortwave transmissivity are further reduced, supporting the modeling by Hardy et al. (2004) and Essery et al. (2008a). This is of particular importance if the aim is to estimate snowpack or forest energy balance over a longer time period. However, modeling daily snowpack energy balance is likely to require data from a larger number of sensors at high temporal resolution and this number is likely to be greater with increased heterogeneity of the canopy. For example, Tribbeck et al. (2006) found that an array of nine radiometers were insufficient to obtain a smooth comparison between modeled solar radiation data on days of high insolation. Link et al. (2004) also determined that increasing the number of sensors improved measurement accuracy, particularly in discontinuous canopies and at high solar angles. The selection of position for the pyranometers in future studies therefore requires

some consideration, as the frequency and duration of sun-flecks can have substantial hydrological and biological significance (Hardy et al. 2004; Pearcy 1988).

With ten sensors in a stationary linear configuration parallel to the moving rail, both configurations captured similar shortwave transmissivity patterns throughout the four analysis periods. However, when the size of the stationary linear configuration was reduced to only three sensors, success in measuring similar patterns to the rail was reduced. Stationary linear configurations have been used in previous studies to capture incoming shortwave and longwave radiation in reference to forest discontinuities (e.g. Essery et al. 2008a; Lawler and Link 2011). Results from the comparisons in this study show that a single moving radiometer can have the same success in capturing spatial variations in shortwave transmission across a small gap in the canopy and can obtain data at a higher spatial resolution (i.e. every 20 cm along the rail) than a stationary array of radiometers. Additionally, it has been shown that when spatially averaged values at a time resolution of less than a day are required, a single or even a small number of stationary radiometers are not adequate to achieve this resolution and quality of data (Vrugt et al. 2002). The rail set-up in this study is also self-cleaning and heated, site maintenance is less labor intensive and radiation data are available immediately following snowfall and precipitation events.

The radiometer locations in the distributed configurations in this study were manually subjectively chosen with the aim of having a similar range of SVFs as the moving rail and linear configurations. The aim of this was to assess how all three configurations capture the spatial variation in sub-canopy incoming radiation caused by the same canopy structure. Locations of the radiometers were therefore chosen with prior knowledge of the canopy structure, a practice that is not commonly adopted when establishing sub-canopy distributed configurations. Even with this knowledge of canopy structure, SVFs in the distributed array had a wider range than those in the linear due to the single larger value

of 0.09. This shows that when arrangements of distributed radiometers are placed using a method with no prior knowledge of the canopy structure in order to reduce human-induced bias, such as those in Pomeroy et al. (2009) or Reid et al. (2014), they may fail to capture the full range of SVFs. This then limits the ability to characterize the sub-canopy radiative regime, which has implications for distributed modeling of longwave and shortwave radiation contribution to snowmelt.

CONCLUSIONS

This study compared incoming shortwave and longwave radiation measurements from three radiometer configurations (stationary distributed, stationary linear, and moving linear) during different sky conditions across an annual range of solar angles. Smaller numbers of radiometers in the stationary configurations were further investigated for differences in measured spatial and temporal variability in incoming shortwave and longwave radiation. The three configurations of radiometers captured similar measurements of longwave enhancement throughout all four seasons. The changes in mean differences from the larger to the smaller configurations adds to the findings of Link et al. (2004), who determined that arrays of around ten pyranometers can produce reasonable estimates of daily sub-canopy radiation. Results from this study indicate that for analysis of sub-canopy incoming shortwave radiation at higher than daily temporal resolutions, an array with a larger number (e.g. n=10) of pyranometers is recommended to capture the sub-canopy spatial and temporal variability of shortwave radiation. However, for longer-term studies less interested in daily variations or in canopy environments similar to that in this study, an array of fewer pyranometers (e.g. n=3) can be sufficient to capture sub-canopy variability. Additional findings in this study show that at this site with SVFs between 0.02 and 0.05, a single stationary pyrgeometer captures a similar spatial variation as measurements from a moving pyrgeometer averaged along a 10 meter rail over the same time period. However, for studies investigating longwave enhancement at close proximity to tree trunks,

406 in sparse canopies or in canopy discontinuities, either a moving array or a stationary array with
407 multiple sensors is recommended.

408 Mean differences from the three comparisons show that the spatial variability of shortwave
409 transmissivity had strong seasonal variation whereas differences in measurements of longwave
410 enhancement between configurations were less seasonally dependent. Measurements of shortwave
411 transmissivity showed greater disparities during periods of higher sun angles, however, mean
412 differences were below 3% in all comparisons. Spatially averaged transmissivity measurements from
413 10 pyranometers over 10-minute periods can therefore be expected to, on average, measure within
414 ±3%, with smaller differences expected during periods of lower solar angles or over larger averaging
415 periods. The results of the three comparisons of shortwave transmissivity measurements by the three
416 configurations presented in this study can therefore be taken to represent the threshold of sub-canopy
417 noise that can be expected when using data from different radiometer configurations in forest
418 canopies of densities similar to that of Seehornwald.

419

420 **ACKNOWLEDGEMENTS**

421 The authors would like to thank Bruno Fritschi for the development, construction and maintenance of
422 the rail, as well as Richard Essery, Tim Link and Tim Reid for their help in establishing the
423 radiometer comparison site, Dave Moeser for assistance with site set-up and supplying the LiDAR
424 data, and Saskia Gindraux and Franziska Zieger who assisted in site maintenance throughout the
425 measurement periods. Funding for the CMP3 and CGR3 radiometers used in this study were
426 provided to N. Rutter from the UK's Natural Environment Research Council (NERC) Grant number

NE/H008187/1. We would also like to thank Jessica Lundquist and two other anonymous reviewers whose comments improved this paper.

REFERENCES

Baldocchi, D. D., B. E. Law, and P. M. Anthoni, 2000: On measuring and modeling energy fluxes above the floor of a homogeneous and heterogeneous conifer forest. *Agricultural and Forest Meteorology*, **102,** 187-206.

Black, T. A., J.-M. Chen, X. Lee, and R. M. Sagar, 1991: Characteristics of shortwave and longwave irradiances under a Douglas-fir forest stand. *Canadian Journal of Forest Research*, **21,** 1020-1028.

Blanken, P., T. Black, H. Neumann, G. Den Hartog, P. Yang, Z. Nesic, and X. Lee, 2001: The seasonal water and energy exchange above and within a boreal aspen forest. *Journal of Hydrology*, **245,** 118-136.

Brown, G. W., 1973: Measuring transmitted global radiation with fixed and moving sensors. *Agricultural Meteorology*, **11,** 115-121.

Chazdon, R. L., K. Williams, and C. B. Field, 1988: Interactions between crown structure and light environment in five rain forest Piper species. *American Journal of Botany***,** 1459-1471.

Chen, J., P. Blanken, T. Black, M. Guilbeault, and S. Chen, 1997: Radiation regime and canopy architecture in a boreal aspen forest. *Agricultural and Forest Meteorology*, **86,** 107-125.

Ellis, C., J. Pomeroy, and T. Link, 2013: Modeling increases in snowmelt yield and desynchronization resulting from forest gap-thinning treatments in a northern mountain headwater basin. *Water Resources Research*, **49,** 936-949.

Essery, R., J. Pomeroy, C. Ellis, and T. Link, 2008a: Modelling longwave radiation to snow beneath forest canopies using hemispherical photography or linear regression. *Hydrological Processes*, **22,** 2788-2800.

Essery, R., and Coauthors, 2008b: Radiative transfer modeling of a coniferous canopy characterized by airborne remote sensing. *Journal of Hydrometeorology*, **9,** 228-241.

Essery, R., and Coauthors, 2009: SNOWMIP2: An evaluation of forest snow process simulations. *Bulletin of the American Meteorological Society*, **90,** 1120-1135.

Fröhlich, C., 1977: World radiometric reference. *Commission for Instruments and Methods of Observation. Abridged final report of the seventh session, CIMO-VII, WMO*.

Harding, R., and J. Pomeroy, 1996: The energy balance of the winter boreal landscape. *Journal of Climate*, **9,** 2778-2787.

Hardy, J., R. Davis, R. Jordan, W. Ni, and C. E. Woodcock, 1998: Snow ablation modelling in a mature aspen stand of the boreal forest. *Hydrological Processes*, **12,** 1763-1778.

Hardy, J., R. Melloh, G. Koenig, D. Marks, A. Winstral, J. Pomeroy, and T. Link, 2004: Solar radiation transmission through conifer canopies. *Agricultural and Forest Meteorology*, **126,** 257-270.

Law, B. E., A. Cescatti, and D. D. Baldocchi, 2001: Leaf area distribution and radiative transfer in open-canopy forests: implications for mass and energy exchange. *Tree Physiology*, **21,** 777-787.

Lawler, R. R., and T. E. Link, 2011: Quantification of incoming all-wave radiation in discontinuous forest canopies with application to snowmelt prediction. *Hydrological Processes*, **25,** 3322-3331.

Link, T. E., D. Marks, and J. P. Hardy, 2004: A deterministic method to characterize canopy radiative transfer properties. *Hydrological Processes*, **18,** 3583-3594.

Lundquist, J. D., S. E. Dickerson-Lange, J. A. Lutz, and N. C. Cristea, 2013: Lower forest density enhances snow retention in regions with warmer winters: A global framework developed from plot-scale observations and modeling. *Water Resources Research*, **49,** 6356-6370.

Nobis, M., and U. Hunziker, 2005: Automatic thresholding for hemispherical canopy-photographs based on edge detection. *Agricultural and Forest Meteorology*, **128,** 243-250.

474 Pearcy, R. W., 1988: Photosynthetic utilisation of lightflecks by understory plants. *Functional Plant*
475 *Biology*, **15,** 223-238.
476 Pomeroy, J. W., D. Marks, T. Link, C. Ellis, J. Hardy, A. Rowlands, and R. Granger, 2009: The
477 impact of coniferous forest temperature on incoming longwave radiation to melting snow.
478 *Hydrological Processes*, **23,** 2513-2525.
479 Reid, T., R. Essery, N. Rutter, and M. King, 2014: Data-driven modelling of shortwave radiation
480 transfer to snow through boreal birch and conifer canopies. *Hydrological Processes*, **28,** 2987-3007.
481 Reifsnyder, W. E., G. Furnival, and J. Horowitz, 1972: Spatial and temporal distribution of solar
482 radiation beneath forest canopies. *Agricultural Meteorology*, **9,** 21-37.
483 Rowlands, A., J. Pomeroy, J. Hardy, D. Marks, K. Elder, and R. Melloh, 2002: Small-scale spatial
484 variability of radiant energy for snowmelt in a mid-latitude sub-alpine forest. *Proceedings of the 59th*
485 *Eastern Snow Conference*, 109-117.
486 Schleppi, P., M. Conedera, I. Sedivy, and A. Thimonier, 2007: Correcting non-linearity and slope
487 effects in the estimation of the leaf area index of forests from hemispherical photographs.
488 *Agricultural and Forest Meteorology*, **144,** 236-242.
489 Sicart, J. E., R. L. H. Essery, J. W. Pomeroy, J. Hardy, T. Link, and D. Marks, 2004: A Sensitivity
490 Study of Daytime Net Radiation during Snowmelt to Forest Canopy and Atmospheric Conditions.
491 *Journal of Hydrometeorology*, **5,** 774-784.
492 Stähli, M., T. Jonas, and D. Gustafsson, 2009: The role of snow interception in winter-time radiation
493 processes of a coniferous sub-alpine forest. *Hydrological Processes*, **23,** 2498-2512.
494 Tribbeck, M. J., R. J. Gurney, and E. M. Morris, 2006: The Radiative Effect of a Fir Canopy on a
495 Snowpack. *Journal of Hydrometeorology*, **7,** 880-895.

Vrugt, J. A., W. Bouten, S. C. Dekker, and P. A. Musters, 2002: Transpiration dynamics of an Austrian Pine stand and its forest floor: identifying controlling conditions using artificial neural networks. *Advances in Water Resources*, **25,** 293-303.

Woo, M.-k., and M. A. Giesbrecht, 2000: Simulation of snowmelt in a subarctic spruce woodland: 1. Tree model. *Water Resources Research*, **36,** 2275-2285.

CAPTIONS

Table 1: Summary data for each analysis period

Figure 1: a) Birds eye view of field site showing location of rail and linear array with reference to locations of radiometers from the distributed array on the forest floor. Filled points denote pyranometers and open points denote pyrgeometers. Radiometers in the distributed configuration are in blue and the linear configuration is in red. Green circles represent tree crown positions determined by aerial LiDAR data. Numbering of radiometers indicates those selected in the analysis with 3 pyranometers and 1 pyrgeometer. b) Photograph showing the position of the radiometers in the linear configuration. Photograph looks south along the rail. The CNR1 attached to the rail is leveled at the same height as the stationary radiometers so they do not influence each other.

Figure 2: Scatterplots showing differences in measurements of shortwave transmissivity (a, c, e) and longwave enhancement (b, d, f) for the distributed and rail comparison (a, b), the stationary distributed and linear comparison (c, d) and the linear and rail comparison (e, f) across the four study periods.

Figure 3: Summary of results of statistical analysis of mean difference (left column), coefficient of variation (middle column) and correlation using Pearson's *R* (right column) for the differences in measurements of shortwave transmissivity (top row) and longwave enhancement (bottom row) across autumn (A), winter (W), spring (Sp) and summer (Su). Mean differences are expressed as a

523 percentage of transmissivity/enhancement. All *R-value*s were statistically significant at 99%
524 confidence. X denotes lack of data in the LW comparisons involving the rail in Autumn.

525

526 Figure 4: As Figure 2 but for three pyranometers and one pyrgeometer in each of the two stationary
527 configurations.

528

529 Figure 5: Mean difference and coefficient of variation for the comparisons when the number of
530 sensors is reduced from ten to three pyranometers and four to one pyrgeometer.

531

532

532

533 **TABLES**

534 Table 2: Summary data for each analysis period

Analysis Period	Start date	Midday solar angle	End date	Midday solar angle
Autumn	2 Oct 2013	38.7º	10 Oct 2013	36.0º
Winter	12 Dec 2013	20.2º	24 Dec 2013	19.8º
Spring	7 May 2014	59.6º	14 May 2014	61.3º
Summer	14 June 2014	66.4º	23 June 2014	66.6º

535

536

FIGURES

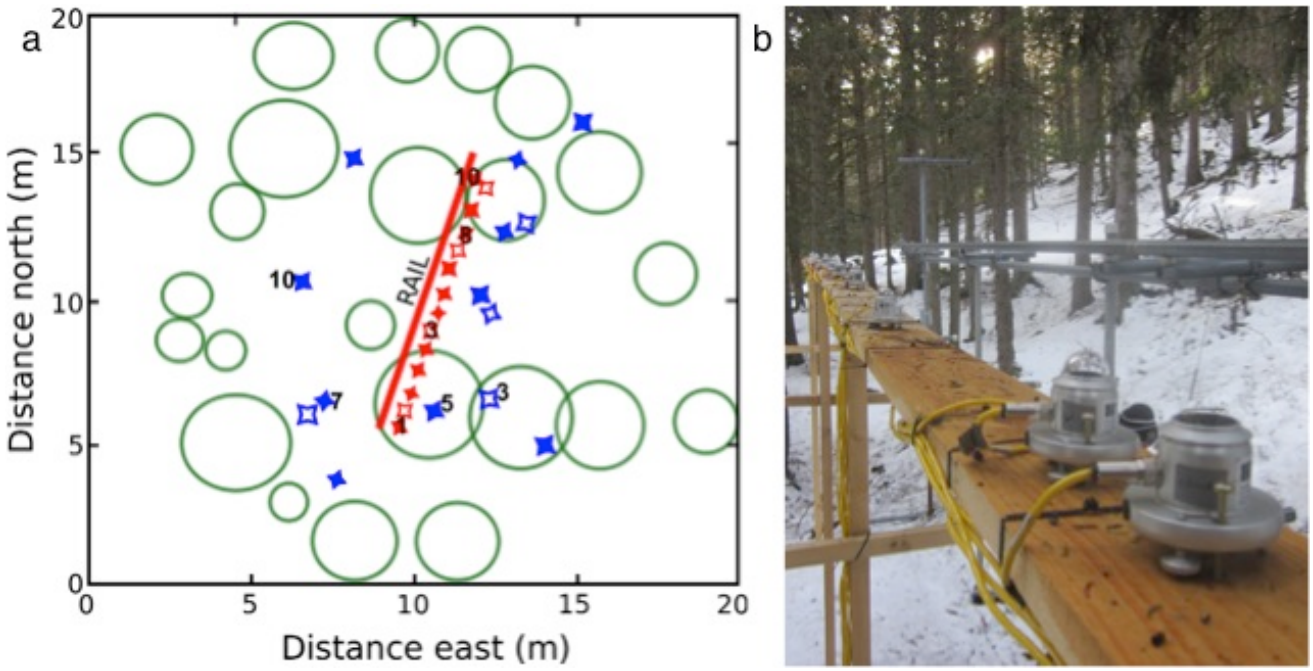

Figure 4: a) Birds eye view of field site showing location of rail and linear array with reference to locations of radiometers from the distributed array on the forest floor. Filled points denote pyranometers and open points denote pyrgeometers. Radiometers in the distributed configuration are in blue and the linear configuration is in red. Green circles represent tree crown positions determined by aerial LiDAR data. Numbering of radiometers indicates those selected in the analysis with 3 pyranometers and 1 pyrgeometer. b) Photograph showing the position of the radiometers in the linear configuration. Photograph looks south along the rail. The CNR1 attached to the rail is leveled at the same height as the stationary radiometers so they do not influence each other.

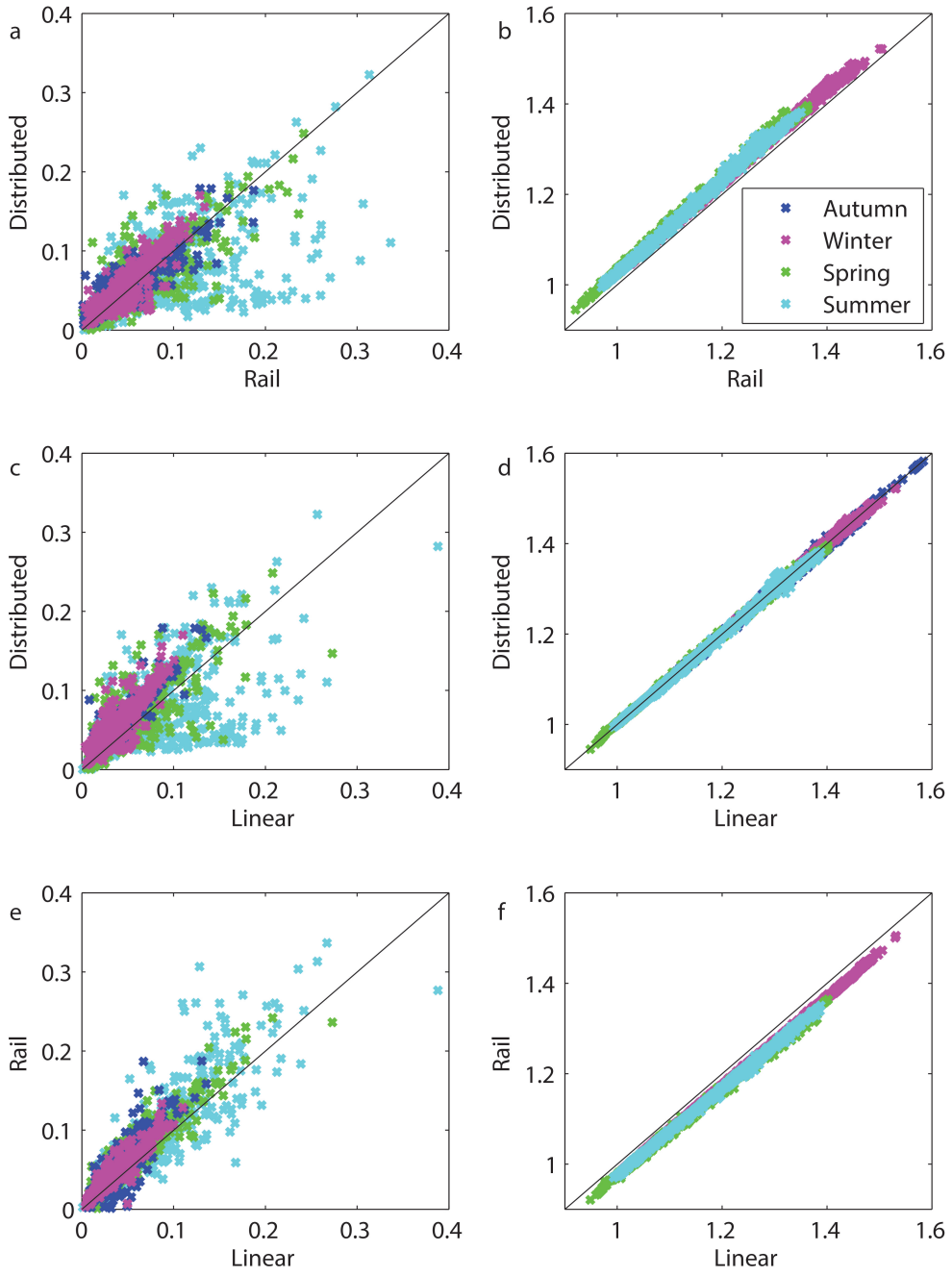

547

548 Figure 5: Scatterplots showing differences in measurements of shortwave transmissivity (a, c, e) and
549 longwave enhancement (b, d, f) for the distributed and rail comparison (a, b), the stationary
550 distributed and linear comparison (c, d) and the linear and rail comparison (e, f) across the four study
551 periods.

552

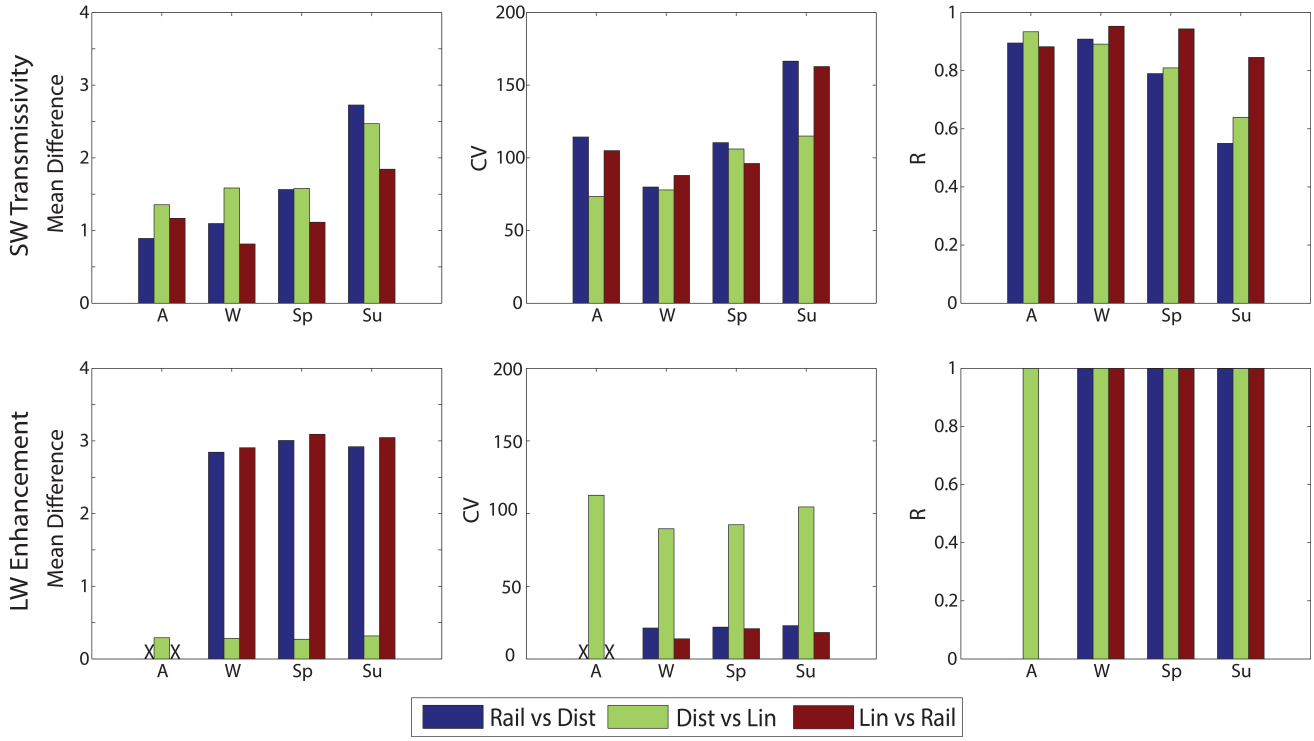

552

553 Figure 6: Summary of results of statistical analysis of mean difference (left column), coefficient of
554 variation (middle column) and correlation using Pearson's *R* (right column) for the differences in
555 measurements of shortwave transmissivity (top row) and longwave enhancement (bottom row) across
556 autumn (A), winter (W), spring (Sp) and summer (Su). Mean differences are expressed as a
557 percentage of transmissivity/enhancement. All *R-value*s were statistically significant at 99%
558 confidence. X denotes lack of data in the LW comparisons involving the rail in Autumn.

559

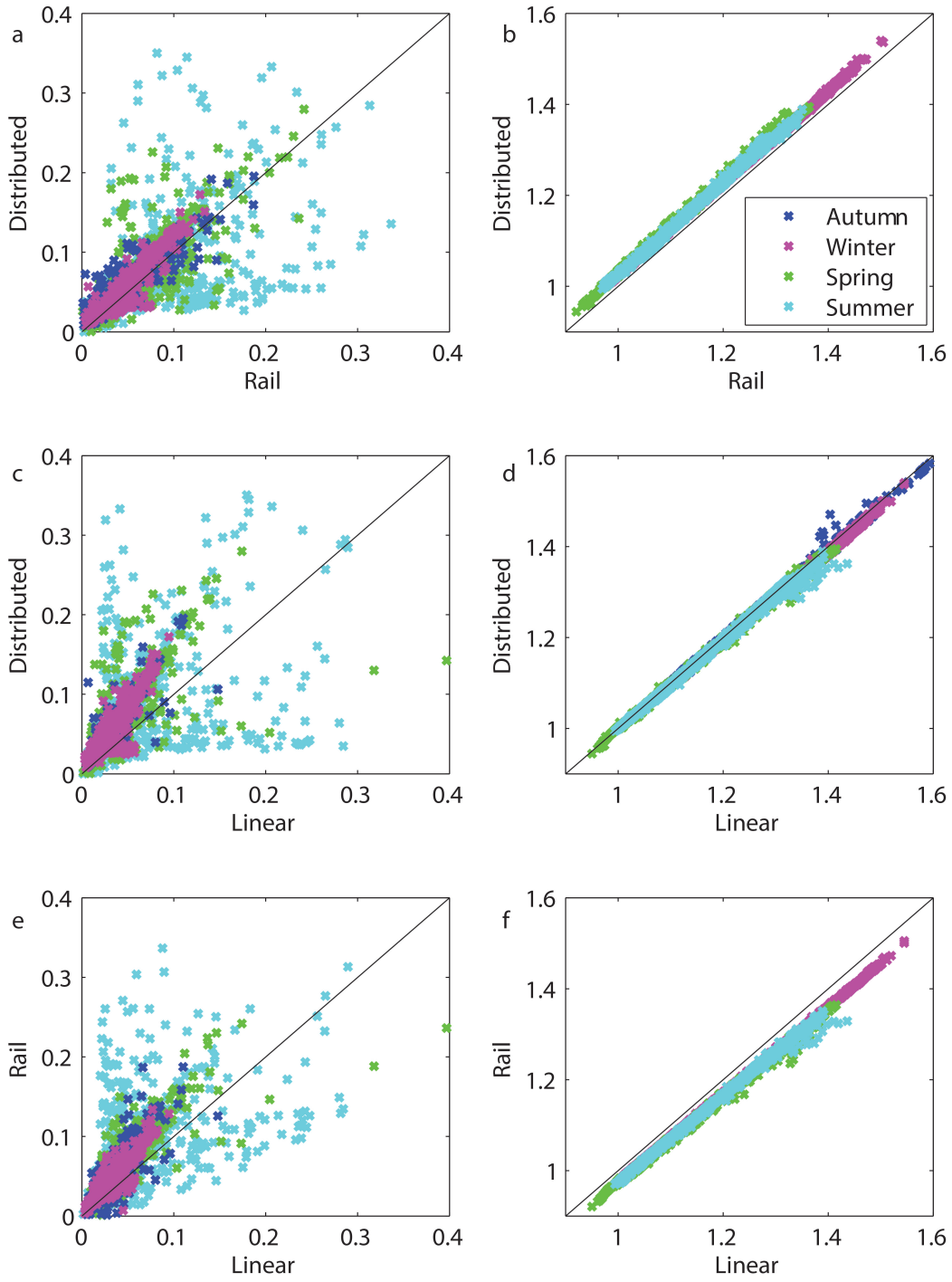

559

560 Figure 7: As Figure 2 but for three pyranometers and one pyrgeometer in each of the two stationary

561 configurations.

562

562

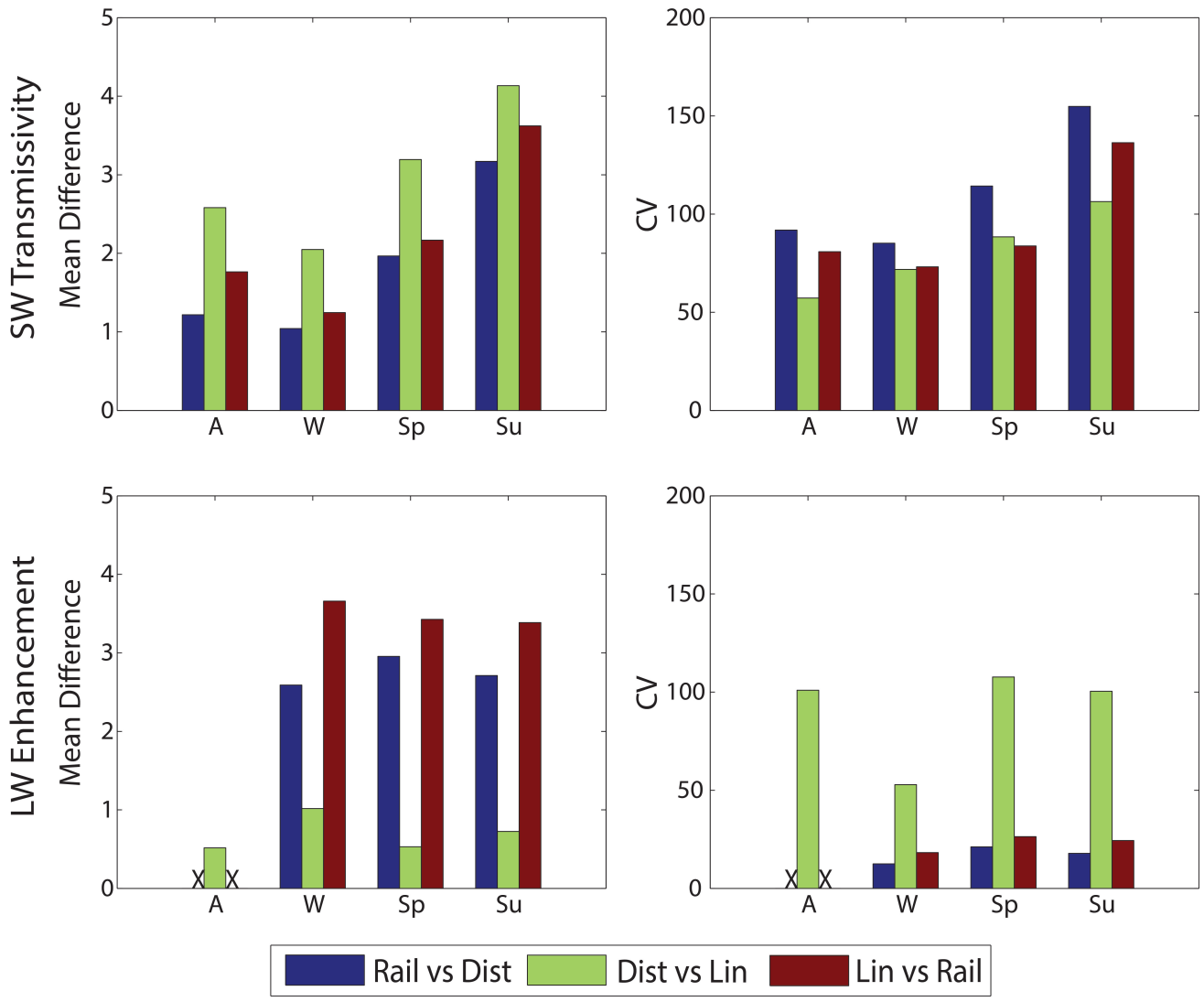

563

564 Figure 8: Mean difference and coefficient of variation for the comparisons when the number of
565 sensors is reduced from ten to three pyranometers and four to one pyrgeometer.